Experiments in Fluids 28 (2000) 116–127 © Springer-Verlag 2000

Laboratory measurement of suspended sediment concentration using an Acoustic Concentration Profiler (ACP)

D. M. Admiraal, M. H. García

Abstract Vertical profiles of suspended sediment concentration have been gathered in a laboratory flume using a 2.25 MHz acoustic transducer. The acoustic concentration profiler (ACP) was calibrated in a vertical duct for homogeneous concentrations of two uniformly sized sediments. The transducer was then transferred to a 6 m horizontal flume where concentration profiles were measured in steady and unsteady flows. For the steady flow tests, concentration measurements made with the ACP and with suction samplers are compared. The results demonstrate that the ACP provides an accurate method of non-intrusively measuring sediment concentrations of more than 2.5% by volume.

1 Introduction

Measurement of the concentration of suspended sediment in a water column has long been important in fluvial hydraulics. Recently, some applications have made it necessary to measure sediment concentrations in unsteady flows. For example, resuspension of sediment by the passage of large boats has aroused interest because of the possibility of reentrainment of deposited contaminants. Traditional methods of measuring sediment concentration do not work well for unsteady flows. Consequently, acoustic methods are explored in this paper as an alternative for measuring sediment concentrations in unsteady flows.

For useful concentration measurements, the measuring device must have good spatial resolution and a small measuring volume. For two-dimensional flows the spanwise and lengthwise dimensions of the measuring volume are not critical, but its height should be small relative to the thickness of the boundary layer. A small measuring volume height is necessary since most vertical distributions of suspended sediment are nonlinear. In unsteady flows good time response is also required. Necessary time response depends on the level of unsteadiness.

Typical characteristics of three of the more widely used methods of measuring sediment concentration – manual sampling, Optical Back Scatter (OBS), and acoustic back scatter (ACP) – are given in Table 1. Note that specifications given in Table 1 may vary somewhat with instrument design. Only manual sampling provides direct measurements of concentration and can determine sediment size and sediment concentration simultaneously. Using samplers, suspensions of sediment are siphoned out of the flow at velocities that are usually equivalent to what the velocity of the flow at the entrance of the siphoning tube would be if the siphoning tube were not present (isokinetic sampling). Unfortunately, manual sampling is flow intrusive, requires sample processing (samples must be dried and weighed), and has poor temporal resolution. Manual samplers are discussed in more detail by Bosman et al. (1987), Winterstein and Stefan (1983), Coleman (1981), and van Rijn (1981).

A manual sampler was used to calibrate the ACP used in the present work. Since volumetric sediment concentrations are directly measured, results gathered with the sampler should be relatively accurate. However, as shown by Bosman et al. (1987), accuracy of manual samplers varies with sampling rate, sediment size, and the angle of the sampler relative to the flow velocity. Measuring concentration quickly and accurately in time-varying flows requires the use of instruments with better temporal resolution than manual samplers. Of the three methods shown in Table 1, ACPs are the least flow intrusive. ACPs also have good temporal resolution and, unlike OBS sensors, can gather an entire vertical concentration profile in one reading. In this paper, the performance of an ACP is investigated, and resulting measurements are shown for both steady and unsteady flows.

2 Acoustic concentration profilers (ACPs)

Acoustic Concentration Profilers (ACPs) transmit pressure pulses at frequencies of more than 1 MHz through water. A fraction of each pulse is reflected by suspended sediment and is returned to the transducer. The strength of the return signal is directly related to the concentration of sediment in the water. The velocity of the transmitted pulse is the speed of sound in water; so if the strength of the return signal is measured as a function of time, a vertical profile of the

Received: *24 September 1998*/*Accepted*: *12 April 1999*

D. M. Admiraal, M. H. García
Hydrosystems Laboratory
Department of Civil and Environmental Engineering
University of Illinois at Urbana-Champaign
205 North Mathews Ave.
Urbana, IL 61801, USA

Correspondence to: D. M. Admiraal

The support of the U.S. Army Corps of Engineers, Waterways Experiment Station (Grants DAAH04-96-1-0132 and DACW39-95-K-0101) and the U.S. Office of Naval Research (Grant N0014-93-1-0044) is gratefully acknowledged. The authors thank José Rodríguez for his help with the experiments. Finally, the authors are especially thankful for the generosity and helpfulness of Alex Hay.

Table 1. Typical characteristics of three methods of measuring suspended sediment concentration

Characteristic	Manual samplers	Optical back scatter	Single frequency acoustic back scatter (ACP)
Sampling rate	~0.1 Hz or less	10 Hz	100 Hz*
Temporal resolution	~10 s	~0.1 s	~0.1 s
Measuring volume dimensions	Inlet diameter as small as 2–3 mm	Cone Cone half angle: 15° Cone length: ~25 mm Cone volume: ~1.3 cm^3	Frustum of a cone Frustum height: 7.5 mm Frustum diameter: ~30 mm Frustum volume: ~5 $cm^{3\dagger}$
Intrusiveness	Flow intrusive	Slightly intrusive	Non-intrusive
Measurements per sample	One	One	Multiple readings constitute an entire concentration profile
Calibration requirements	Calibration generally unnecessary	Calibration required using relevant sediment distribution	Calibration required using relevant sediment distribution
Sediment size distribution	Simultaneously measures size distribution and concentration	Sensor can only measure concentration of the sediment distribution used in its calibration	Sensor can only measure concentration of the sediment distribution used in its calibration

*However, multiple samples may be required to obtain a reliable result.
† Diameter and volume of sampling volume vary with distance from the transducer. Height and volume may be reduced substantially by changes in ACP design.

sediment concentration can be obtained. The amount of time that it takes to gather an entire vertical profile is found by multiplying twice the distance from the transducer to the bed by the speed of sound in water. For our experiments, the amount of time required to gather a profile was only about 0.5 ms. This method of measuring concentration is rapid, simple, and can be used in unsteady flows.

Acoustic sensors have been investigated primarily in estuaries and oceanic boundary layers where there are large characteristic lengths (Libicki et al. 1989; Hay and Sheng 1992; Thorne et al. 1996). The height of the ACP's measuring volume depends on the duration of the transmitted pulse. For example, the pulse duration of the ACP presented herein is 10 μs. Since the speed of sound in water is approximately 1500 m/s, the distance that each pulse encompasses is about 1.5 cm. The height of the measuring volume is 1/2 of this distance; in this case 0.75 cm. It is physically possible to decrease the height of the measuring volume by reducing the duration of the transmit pulse. For a 2.25 MHz transducer, a 10 μs pulse has about 20 cycles. Two full amplitude cycles might be enough to capture good concentration measurements, but piezo-electric transducers cannot achieve full output instantaneously and require a small start up time. An estimate of the shortest reliable pulse is about 5 cycles, translating to a pulse duration of about 2.5 μs and a measuring volume height of about 2 mm for a 2.25 MHz transducer. Unfortunately, the design of the ACP used for the current set of tests did not permit a pulse duration of less than 10 μs.

Although the frequency of the ACP described herein is 2.25 MHz, the receiver of the ACP heterodynes the return signal to 455 kHz prior to output, making analog to digital conversion of the output more manageable. Using a high speed analog to digital converter, the entire 455 kHz signal is digitally captured and envelope detected. The output of the ACP is continuous, and the locations of measuring volumes are based on the time at which the output is sampled. The 455 kHz output limits the accuracy of locating the center of a measuring volume with respect to the bed to about 2 mm. Consequently, the spatial resolution of measurements taken with the ACP is no better than 2 mm.

Calibration curves for acoustic sensors are different for different sediment sizes. Recent work by Crawford and Hay (1993) demonstrated that two sensors of different frequency may be used to discern sediment size as well as concentration for non-uniform sediment mixtures. However, Libicki et al. (1989) claim that sensors operating at frequencies upwards of 30 MHz would be necessary to model the range of sediment sizes expected for ocean boundary layer measurements. Frequencies of this magnitude are not very practical for a number of reasons. In this study sediment size distributions were uniform and only one ACP was necessary, but the ACP had to be recalibrated for each sediment size investigated.

The acoustic signal is attenuated as it travels through the water, both by particles in the water and by the water itself. The attenuation caused by the suspended sediment can be ignored for low concentrations, but if the concentration is high enough it must be accounted for. Hay (1991) assumes that attenuation due to particles in the water is negligible when concentrations are less than one percent by volume. Equation (1) has been given by Fisher and Simmons (1977) for calculating the attenuation of sound in water, α_w.

$$\alpha_w = (55.9 - 2.37T + 4.77 \times 10^{-2}T^2 - 3.48 \times 10^{-4}T^3)\, 10^{-15} f^2 \times (1 - 3.84 \times 10^{-4}p + 7.57 \times 10^{-8}p^2) \quad (1)$$

where f is the frequency of the transmitted signal in Hz, T is the water temperature in C, and p is the absolute pressure in Atm.

3
ACP operation

The ACP gathers an entire profile of suspended sediment concentration by transmitting a short duration acoustic pulse through the water column. The pulse travels through the insonified area schematically shown in Fig. 1, and is reflected by any discontinuity in the fluid. Reflections of the pulse are sensed by the transducer as a function of time, and the distance from the transducer to the detected discontinuities is related to the time between transmission and detection and the speed of sound in water. An example of the measuring volume detected by the acoustic transducer is also shown in Fig. 1. Because of the radial spreading of the acoustic pulse the measuring volume is best treated with spherical coordinates. The pulse transmitted by the ACP has a pressure amplitude that is dependent on direction. The strongest part of the transmitted pulse is limited to the cone defined by an azimuthal angle of 3°. Beyond the 3° angle the pressure pulse has an intensity at least 3 dB smaller than the maximum pressure intensity. The directivity, D, of the transmitted pulse defines how intense the pressure pulse is in any direction.

Derivations of the equations describing backscattering by suspended sediment particles have been given by Hay (1991), Thorne and Campbell (1992), and Thorne et al. (1993). The equation for the pressure scattered by a single particle, p_s, has been given by Thorne et al. as

$$p_s = a_s p_0 r_0 \frac{D^2}{2r^2} f_m \exp\{\mathrm{i}[2r(k+\mathrm{i}\alpha_w)-\omega t]\} \quad (2)$$

where a_s is the radius of the scattering particle, p_0 is the pressure amplitude of the sound wave at a distance r_0 from the transducer, D is the directivity of the sensor (where D is a function of the angle from the axis of the transducer, θ), r is the distance from the transducer to the particle, f_m is a form function defining the particle's scattering properties, k and ω are the wave number and angular frequency of the incident sound wave, and t is the time.

Eq. (2) can be integrated over the measuring volume insonified by the acoustic pulse. The measuring volume is the frustum of a cone defined by the 3 dB boundary angle described above and by the duration of the transmission pulse. The mean radius of the measuring volume depends on distance from the transducer, and is approximately $r\tan\beta_m$, where β_m is the 3 dB boundary angle. In the current set of experiments measuring volumes are between 25 and 35 cm from the transducer, and the radius of the measuring volume varies between 1.3 and 1.8 cm, respectively.

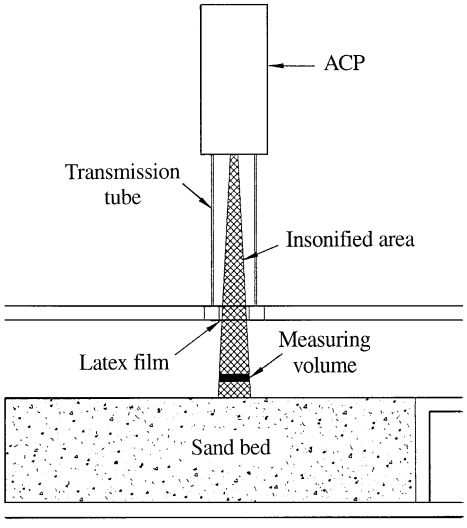

Fig. 1. Variation of ACP measuring volume with distance from transducer

All of the reflections that occur within the measuring volume and return to the transducer at the same time constitute a measurement. Since the leading and trailing edges of the acoustic pulse are the first and last parts of the pulse to arrive at the measuring volume, they define the upper and lower boundaries of the volume. Within the volume, the leading edge of the acoustic pulse is partially reflected off of the particles furthest from the transducer, and the trailing edge of the acoustic pulse is partially reflected off of the particles that are nearest the transducer. In order to return to the transducer at the same time, the reflected fractions of the leading and trailing edges of the pulse must exit the measuring volume simultaneously. Thus, the reflected fraction of the leading edge must travel twice the height of the measuring volume (through the volume and back) by the time the trailing edge enters the measuring volume. Since the leading edge has always traveled a distance of $c\tau$ farther than the trailing edge, the height of the measuring volume is $c\tau/2$, where c is the speed of sound in the water, and τ is the pulse duration.

Therefore, the boundaries of the integral are $r-c\tau/4$, $r+c\tau/4$, and β_m. A sufficiently large number of scatterers is necessary within each measuring volume so that the combined return signals of the individual scatterers produce an incoherent pressure field. The number of scatterers intercepted by one acoustic pulse is not always large enough to return an incoherent pressure field, and to assure reliable results it is often necessary to ensemble average a large number of backscattered signals (Thorne and Campbell 1992; Thorne et al. 1993). Assuming that there are either sufficient scatterers or that a sufficient number of pulses have been ensemble averaged, the ensemble average root-mean-square backscatter pressure, p_{rms}, is given by

$$\langle p_{\mathrm{rms}}\rangle = p_0 r_0 \left(\frac{3M\langle f_m^2\rangle}{16\pi\rho_s a_s}\right)^{1/2} \left(\int_0^{\beta_m}\int_0^{2\pi}\int_{r-\tau c/4}^{r+\tau c/4} \frac{D^4}{r^2} \mathrm{e}^{-4r\alpha_t} \sin\theta \,\mathrm{d}r\,\mathrm{d}\phi\,\mathrm{d}\theta\right)^{1/2} \quad (3)$$

where M is the mass of scatterers per unit volume of fluid, ρ_s is the density of the scatterers, and α_t is the total attenuation coefficient. If τc is significantly smaller than r Eq. (3) can be simplified further to get Eq. (4):

$$\langle p_{\mathrm{rms}}\rangle = \frac{p_0 r_0 (\langle |f_{\mathrm{m}}|^2\rangle^{1/2})}{\psi r} \left(\frac{3\tau c M}{16\rho_s a_s}\right)^{1/2} \left(\int_0^{\beta_m} D^4 \sin\theta \,\mathrm{d}\theta\right)^{1/2} \mathrm{e}^{-2\alpha_t r} \quad (4)$$

where ψ was introduced by Thorne et al. (1993) to adjust the equation if the calculation is being done in the near-field of the transducer instead of the far-field. Eq. (5) can be used to replace the integral term in Eq. (4). According to Thorne et al.

(1993) Eq. (5) is within three percent for $\beta_m < 15^\circ$.

$$\left(\int_0^{\beta_m} D^4 \sin\theta \, \mathrm{d}\theta\right)^{1/2} = \left(\int_0^{\beta_m} \left\{\frac{2J_1(ka_t \sin\theta)}{ka_t \sin\theta}\right\}^4 \sin\theta \, \mathrm{d}\theta\right)^{1/2} \approx \frac{1}{1.05\, ka_t} \tag{5}$$

where J_1 is the first-order Bessel function, and a_t is the radius of the transducer. Combining Eq. (4) and Eq. (5) yields:

$$\langle p_{\mathrm{rms}} \rangle = \frac{p_0 r_0 (\langle |f_m|^2 \rangle^{1/2})}{\psi r} \left(\frac{3\tau c M}{16 \rho_s a_s}\right)^{1/2} \frac{\mathrm{e}^{-2\alpha_t r}}{1.05\, ka_t} \tag{6}$$

The attenuation coefficient α_t is given by:

$$\alpha_t = \alpha_w + \frac{1}{r}\int_0^r \alpha_s \, \mathrm{d}r \tag{7}$$

Here, α_s is the attenuation of the acoustic pulse due to sediment suspended in the water, and is a function of sediment size, sediment type, and concentration (Thorne et al. 1995). The integral in Eq. (7) is necessary since the sediment attenuation coefficient may be different at different locations between the transducer and the measuring volume; this is due to spatial variations in the sediment concentration. The attenuation due to the suspended sediment has been shown to follow the relation given by (Hay 1991; Thorne et al. 1995).

$$\alpha_s = \zeta M \tag{8}$$

where ζ is a constant determined by sediment characteristics.

Since attenuation due to the sediment is dependent on the concentration, calculating concentration profiles for high concentrations is not trivial. If attenuation is known as a function of concentration, the attenuation can be corrected for by first computing the concentration closest to the sensor, then calculating the corresponding attenuation, then calculating the concentration slightly further from the sensor (using the previously calculated attenuation correction), and so on until the entire concentration profile is known.

Thorne et al. (1993) show that the near-field correction ψ is given by

$$\psi = 1 \quad \text{for } r > \frac{\varepsilon \pi a_t^2}{\lambda} \tag{9a}$$

$$\psi = \frac{1}{3}\left[2 + \frac{\varepsilon \pi a_t^2}{\lambda r}\right] \quad \text{for} \quad r < \frac{\varepsilon \pi a_t^2}{\lambda} \tag{9b}$$

where ε is approximately 2, and λ is the acoustic wavelength.

The output voltage of the transducer, v, is related to the incident pressure by a constant (Hay 1991), so that

$$\langle v^2 \rangle = \chi \langle p^2 \rangle \tag{10}$$

where χ is a system sensitivity constant.

A transducer can easily be calibrated using Eqs. (6)–(10). For a given transducer and sediment, p_0, r_0, f_m, k, a_t, a_s and ρ_s are constants, and τc is approximately constant. Eq. (6) can be combined with Eq. (10) and reduced to get

$$\langle v^2 \rangle = C \frac{M}{\psi^2 r^2} \mathrm{e}^{-4\alpha_t r} \tag{11}$$

where C is a constant that can be determined by calibration. For our transducer, a time variable gain amplifier (TVG) corrects the return signal for spherical spreading and attenuation of the signal due to the water. If the measurements are being made in the far-field ψ is 1, and Eq. (12) can be used. The TVG used by our sensor is not exact since it does not account for changes in the water temperature, however variations in the temperature of our calibrations and experiments are not large enough (5°C maximum) to produce substantial error, otherwise temperature correction of the attenuation can be performed

$$\langle v^2 \rangle = CM \mathrm{e}^{-4\int_0^r \alpha_s \, \mathrm{d}r} \tag{12}$$

If concentrations are low enough so that attenuation by the sand is negligible, Eq. (13) can be used. According to Hay (1991) sand attenuation corrections are generally unnecessary for concentrations of less than one percent by volume. However, the importance of correcting for sand attenuation depends on the distance of the measurement from the transducer and the spatial distribution of sand between the transducer and the measurement location.

$$\langle v^2 \rangle = CM \tag{13}$$

In general, the near-field is considered to be in the region where r is less than A/λ (Downing et al. 1995; Hay 1991) where A is the area of the piston transducer. In order to simplify analysis of concentration results measurements were limited to the far-field. The transducer has a diameter of 1.25 cm so the near-field was limited to 19 cm from the transducer. A transmission tube 25 cm in length was used so that all measurements would occur in the far-field (see Fig. 1). The transmission tube also gives the transducer time to stop ringing after it transmits a pressure pulse. (If operation in the near-field is ever necessary, Downing et al. (1995) show how to correct for measurements in that region.)

As shown in Fig. 1, a latex membrane covers the opening of the transmission tube. The film keeps air bubbles out of the transmission tube and limits flow interference. The effect of this membrane is not accounted for in the equations above and would be difficult to account for, but calibration of the sensor has shown that the above equations work quite well to describe the behavior of the transducer despite the presence of the membrane as long as the sensor is calibrated with the membrane in place. The membrane does not have to be made out of latex. For example, Shen and Lemmin (1996) used Mylar windows to separate their sensors from the suspension. In general, however, membranes that are thin and have a low density transmit sound with fewer losses.

The acoustic profiler used in the experiments is the same one used by Hay (1991). The 2.25 MHz profiler is manufactured by Mesotech, Ltd. for measuring distances to submerged objects. Profilers with frequencies of 1 and 5 MHz are also available. The profiler did not need to be modified to measure sediment concentrations since its output is a function of the strength of the return signal of the transmitted acoustic pulse, and the strength of the return signal is a function of the concentration in the measuring volume. The ACP can gather entire profiles at up to 100 Hz though most of the test results presented herein have been gathered at 10 Hz because of computer constraints, namely, hard drive space and speed.

4
Calibration

Before the ACP was used in the experimental flume it was calibrated, and a relation between the output voltage of the ACP and the sediment concentration was determined. Calibration of the ACP is difficult since uniform concentrations of large diameter sediment are difficult to attain. This difficulty is caused by the tendency of the sediment to settle out of suspension wherever the flow is not turbulent enough. Measurement of the actual concentration of the sediment in the calibration procedure is also difficult. Hay (1991) lists a number of calibration methods, including the sediment-laden jet that he used to calibrate his acoustic sensor. Use of a jet was attempted, but a number of difficulties associated with our application were encountered using this method.

In order to overcome the difficulties associated with calibrating the ACP the calibration facility shown in Fig. 2 was built. The calibration duct is 12 cm wide, 16 cm deep, 85 cm long, and is constructed of $\frac{3}{4}''$ Plexiglas. Water circulates through the calibration duct and returns to a holding tank. The holding tank allows bubbles trapped in the water to be released, preventing the suspended air bubbles from causing erroneous measurements. The sediment in the duct bypasses the holding tank so that the concentration in the duct remains nearly constant throughout each test. A sediment sampler is situated just downstream of the location where ACP profiles are gathered.

Care was taken to design the system with high velocities in all places where the sediment is present. High velocities are necessary to keep the sediment in suspension. Keeping the sediment suspended is important so that a uniform concentration of sediment is maintained over the test period. The cross-sectional areas of all the pipes that recirculate the flow are small with respect to the cross-sectional area of the duct so that velocities are kept high. Measurements with the ACP showed that the suspended sediment concentration was uniform for the entire cross section of the duct so concentration only needed to be sampled at one location along the concentration profile.

The ACP was calibrated with the transmission tube attached. This was done since the latex film and transmission tube affect the calibration. Different amounts of sediment were placed in the facility to get different concentrations, and for each concentration measured with the ACP two to three suction samples were gathered. Two different sizes of quartz sand were used in two separate sets of tests. The diameters of the sand were determined from extensive fall velocity tests. Computed sand grain diameters were 120 and 580 μm, and the geometric standard deviations of the sand diameters were 1.10 and 1.14, respectively (A perfectly uniform distribution of sand has a geometric standard deviation of 1, but for practical purposes, geometric standard deviations of 1.3 or less can be considered uniform). Sediment concentration was determined by manually sampling the flow, and the ACP output voltage was recorded. The ratio of sampler intake velocity to mean velocity in the duct was close to one for the 120 μm sand, but was about three for the 580 μm sand. There is a bias error associated with sampling at a velocity ratio other than one, but sampling at a higher velocity was necessary since the coarse sediment had a high tendency to fall out of solution. Samples taken with intake velocity ratios of about one were available during actual experiments to confirm the calibration of the ACP.

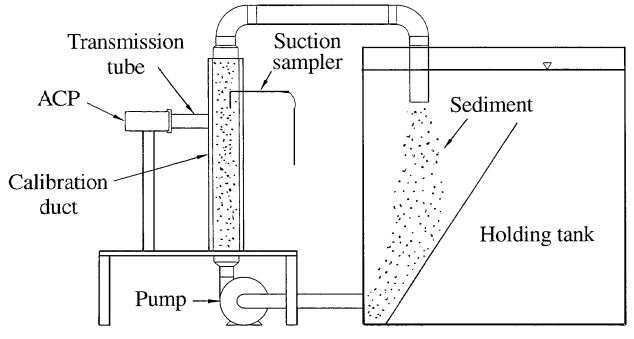

Fig. 2. ACP calibration facility

Mean ACP output voltages were obtained by ensemble averaging a large number of ACP profiles (upwards of 200 profiles). Only the part of the profile nearest the transducer was used to calculate mean voltage so that the effect of attenuation on the calibration results would be minimized. The average voltage did not observably change over the duration of the experiment, indicating that the concentration in the duct was constant with time.

Concentrations measured with the sampler are plotted against the square of the transducer output voltage in Figs. 3 and 4 for the 120 and 580 μm sand grain diameters, respectively. The concentration is given as a function of the average squared output voltage ($\langle v^2 \rangle$) as shown by Eqs. (12) and (13). If data acquisition limitations make it necessary to record a time averaged output voltage instead of the instantaneous output voltage, $\langle v \rangle^2$ must be used instead of $\langle v^2 \rangle$ in Eqs. (12) and (13). For the current set of tests the reduction of accuracy corresponding to this substitution is on the order of 10 percent or less.

An attempt was made to calculate attenuation of the acoustic signal using the calibration data since the ensemble averaged voltages of the entire profile are available. However, it was found that the attenuation correction determined in the calibration facility was not applicable in the resuspension flume. The calibration flume has a very steady concentration, but the resuspension flume has large concentration fluctuations. Hay (1991) points out that if there are large concentration fluctuations, a time-averaged (or ensemble-averaged) attenuation correction will erroneously overcorrect the acoustic output voltage because the correction is non-linear. One way of overcoming this problem is to estimate instantaneous attenuation and use it to correct measured voltages before any averaging is done. With the current setup it is not possible to measure instantaneous concentration for direct comparison with the acoustic signal. Thus, instantaneous attenuation must be determined by optimizing it for all of the instantaneous profiles simultaneously so that the resulting average concentration profiles match those measured with the sampler. The large number of profiles necessary to get a good ensemble average acoustic measurement makes this method time consuming and memory intensive. Instead, the average attenuation associated with high concentration fluctuations was recalculated in the resuspension flume using suction samples gathered during the actual experiments.

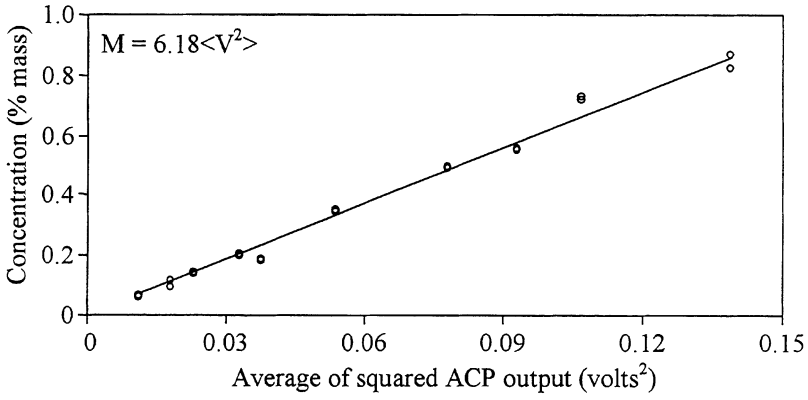

Fig. 3. ACP calibration curve for 120 μm diameter sediment

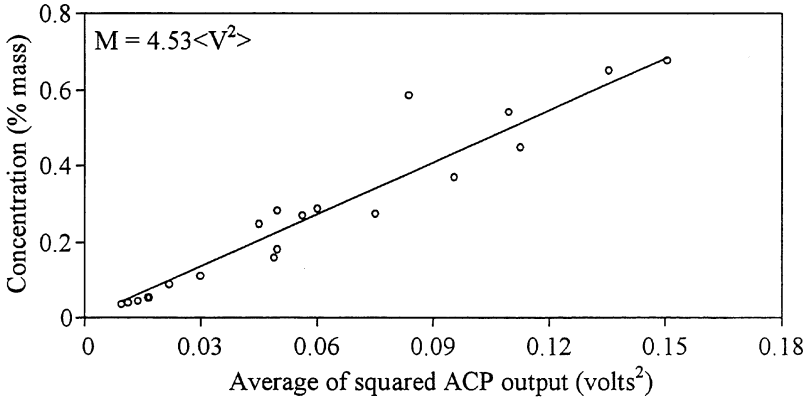

Fig. 4. ACP calibration curve for 580 μm diameter sediment

5
Sources of measurement uncertainty

Data gathered with the ACP is subject to various sources of error. Some sources of error include the presence of air bubbles, variations in water temperature and sand concentration, and analog to digital conversion of the output signal. In this section, sources of uncertainty are examined for the ACP measurements presented in this paper. Some of the measurement errors are not so easily determined. Nevertheless, an estimate of the accuracy of the ACP measurements is given at the end of the section. Calculations of the propagation of errors follow the standard error method shown in Eq. (14). In Eq. (14), $u = f(x_1, x_2, \ldots, x_n)$ where x_1 through x_n represent n independent measured variables, and f is a function.

$$S_u = \left[\left(\frac{\partial u}{\partial x_1} S_{x_1} \right)^2 + \left(\frac{\partial u}{\partial x_2} S_{x_2} \right)^2 + \cdots + \left(\frac{\partial u}{\partial x_n} S_{x_n} \right)^2 \right]^{1/2} \tag{14}$$

S_u represents the measurement uncertainty of u, and S_{x_1} through S_{x_n} represent the measurement uncertainties of the variables x_1 through x_n, respectively.

Equation (11) gives the output of the ACP as a function of mass concentration, distance from the transducer, and total attenuation. Uncertainty of the ACP output given by Eq. (11) can be determined by finding the uncertainties associated with C, M, r, ψ, and α_t. Eq. (15) defines C in terms of measured variables; the equation was derived using Eqs. (6), (10), and (11):

$$C = \chi \left[p_0^2 r_0^2 \langle |f_m|^2 \rangle \left(\frac{3\tau c}{16 \rho_s a_s} \right) \frac{1}{1.05^2 k^2 a_t^2} \right] \tag{15}$$

Uncertainties associated with χ, k, a_t, p_0, r_0, and f_m are negligible, and since the same sediment is used in the calibration and experiments, a_s and ρ_s do not significantly change the uncertainty. The primary sources of uncertainty associated with C are due to τ and c. Variation in the pulse width is estimated to be about one wavelength of the transducer frequency (2.25 MHz), resulting in an uncertainty of about 4%. The uncertainty of the speed of sound in water is about 1.5%, but can be reduced if changes in temperature are accounted for. The overall uncertainty associated with C is about 5%.

Measurement of the distance r is based on c and t, and the uncertainty associated with r is due to time measurement error and variations in the speed of sound. The overall uncertainty of r is about 1.5%. Since all the measurements were taken in the far-field the uncertainty associated with ψ is negligible.

The attenuation coefficient, α_w, varies with temperature as shown by Eq. (1). Over the range of temperatures observed in the experiments α_w varies by as much as 25%. However, the resulting uncertainty of the exponential term in Eq. (11) is only about five percent near the sand bed (error associated with attenuation is highest furthest from the sensor). For high concentrations of sand the uncertainty of α_s can also be important. However, uncertainty due to the sand attenuation

must be calculated on a case by case basis since error associated with the attenuation increases with concentration and distance from the transducer; this is because attenuation of the signal is cumulative (as shown by the integral in Eq. (7)). For the tests presented in this paper the uncertainty due to attenuation appears to be small compared to other sources of uncertainty, and it is ignored in the calculation of the overall uncertainty.

Finally, the uncertainty of M can be calculated from the uncertainty of the sediment samples taken during the calibration procedure. Multiple samples taken during each calibration test show variability between individual measurements. The standard deviation of measurements taken during each test was about four percent for the 120 μm sand and about 8% for the 580 μm sand. Differences between the sampling velocity and flow velocity cause additional error, since samples are not always isokinetic. The uncertainty caused by incorrect sampling velocities was estimated to be about five percent for the 120 μm sand and about 10% for the 580 μm sand. The ramifications of sampling non-isokinetically are more significant for coarse sands than for fine sands. The resulting uncertainty of M is about seven percent for the 120 μm sand and about 13% for the 580 μm sand. Improving accuracy of the sediment samples taken during the calibration procedure is the best way to further improve accuracy of the ACP measurements.

The overall uncertainty associated with the squared ACP output as found from Eq. (11) is about 10% for the 120 μm sand and about 15% for the 580 μm sand. The A/D board used to detect the ACP output has only eight bits of resolution (A high frequency board was required to analyze the ACP output, and resolution had to be sacrificed for a higher sampling rate.) Voltage measurements are very inaccurate at low output voltages. In addition, noise caused by suspended air bubbles interfere with low concentration measurements. These two sources of error are large for tests with concentrations of less than about 0.1% by mass. However, these sources of error are small for higher sand concentrations, and most of the tests had significantly higher concentrations.

The wavelength of the 455 kHz output signal limits the accuracy of distance measurements to about 4 mm. Distance measurements are necessary for finding the locations of measuring volumes with respect to the bed. When finding the location of the bed, the acoustic pulse must travel to the bed and back, and the distance measured is always twice the distance to the bed. Consequently, the uncertainty associated with locating the bed and measuring volumes is one half the uncertainty of the total distance traveled by the acoustic pulse, or about 2 mm.

Finally, there is also error caused by misalignment of the ACP and the transmission tube. The ACP had to be separated from the transmission tube when moving the ACP from the calibration facility to the experimental flume, resulting in possible misalignment of the ACP. Misalignment error can be substantial since reflections off of transmission tube surfaces are large. Consequently, care was taken to realign the ACP as accurately as possible. The magnitude of the error is not easily estimated; so in situ sediment samples were taken to confirm the accuracy of the ACP. Better design of the apparatus would allow the ACP and transmission tube to remain intact between calibration and measurements and could virtually eliminate the error.

6 Experiments

Flow experiments were performed in the flume shown in Fig. 5. The location of the ACP is also shown in the figure, and is approximately 5 m downstream of the entrance of the flume. The ACP is shown mounted above the flow channel on the water filled sound transmission tube. The flume itself consists of a 30 cm wide, 10 cm high rectangular duct constructed of Plexiglas, a 2 m high head tank, and a large volume tailbox. The duct also has a moveable sediment bed as shown in Fig. 5. The sediment bed has a depth of approximately 12.5 cm. The sediment in the flume is not recirculated, and during test runs a scour hole develops at the inlet of the flume. However, the scour hole is filled in before the start of each test run, and during the tests bed elevation remains nearly constant over the 3 m region of bed upstream of the sensors. The maximum variation of the bed elevation within this region is about 3 mm, and bedforms were not observed in any of the tests.

The head at the upstream end of the channel is kept nearly constant at 2 m above the channel centerline. At the downstream end of the channel the discharge is adjusted with a computer controlled valve. The computer that controls the flow valve also controls the triggering system and keeps the ACP synchronized with the flow conditions. The triggering system is necessary so that results from multiple runs can be easily ensemble averaged.

A large number of tests were performed in which the velocity in the duct was increased from zero to a plateau and then kept steady for a period of time. During the steady portion of some of these runs sediment samples were extracted from the flow. The samples were collected at heights of 1, 2 and 3 cm above the bed. Test conditions for the ten tests are given in Table 2. Calibration results presented in the previous section are verified by comparing extracted sediment samples with corresponding ACP measurements. In addition, for the higher concentrations the effects of attenuation are determined.

Figure 6 is a comparison of the data measured with the ACP and the data gathered with the suction samplers for the 120 μm diameter sand steady flow tests. Concentrations measured with the ACP were calculated with and without attenuation taken into account. The attenuation constant, ζ, was calculated by minimizing the error between the suction samples and the ACP data. ζ was found to be 0.0193 when a value of 1/6.18 was used for C. Agreement between the sampled data and the ACP data can be improved further if C is optimized along with ζ.

Figure 7 is a comparison of the data measured with the ACP and the data gathered with the suction samplers for 580 μm diameter sand steady flow tests. Attenuation did not need to be corrected in these flow tests since the concentrations were only high near the bed. If attenuation was important sampled concentrations would likely be higher than the measured concentrations. Consequently, Eq. (13) was used to evaluate the concentration from the measured voltages.

Results shown for the 580 μm sediment have more scatter than results shown for the 120 μm sediment. There are three reasons for this: First, the ACP does much better when measuring high concentrations than low concentrations since

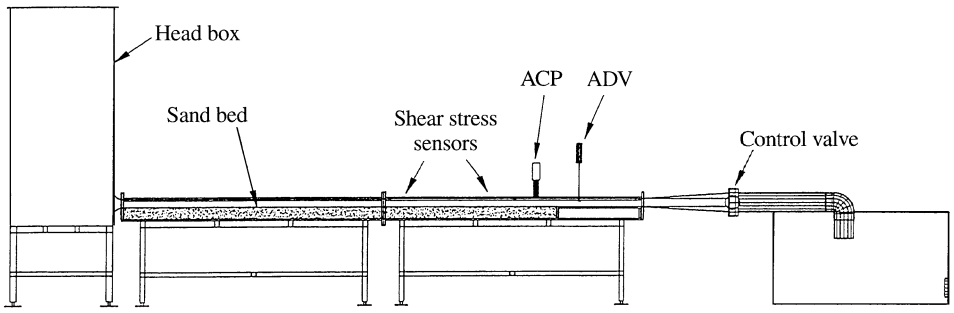

Fig. 5. Side view of the experimental resuspension flume

Table 2. Steady flow test conditions

Test	Sand diameter (μm)	R_{ep}	Centerline velocity (cm/s)	u'_* (m/s)
1a	120	4.9	69.0	0.031
1b	120	4.9	78.7	0.038
1c	120	4.9	90.4	0.040
1d	120	4.9	101.8	0.050
1e	120	4.9	112.7	0.056
2a	580	51	120.3	0.075
2b	580	51	134.4	0.077
2c	580	51	147.2	0.085
2d	580	51	161.9	0.092
2e	580	51	173.3	0.099

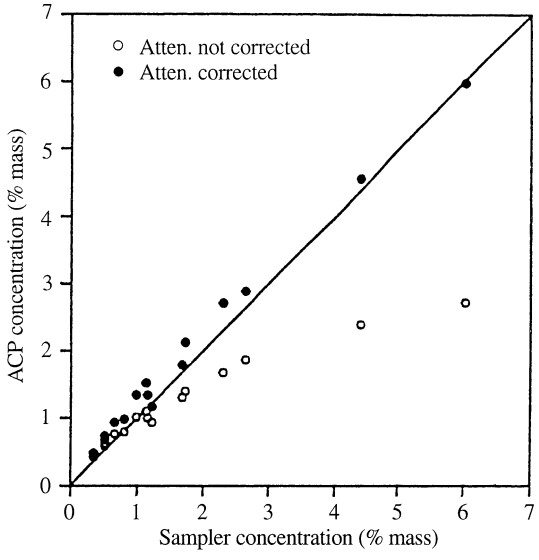

Fig. 6. Comparison of concentrations gathered with the ACP and the suction samplers with and without the attenuation corrected. 120 μm sand grain diameter

noise caused by suspended air bubbles and contaminants has less of an effect on the results for the high concentrations. Second, during the 580 μm sediment tests the gradient of the sediment concentration profile is much steeper near the bed, making it more difficult to get an accurate reading of concentration. Finally, vertical distributions of 580 μm

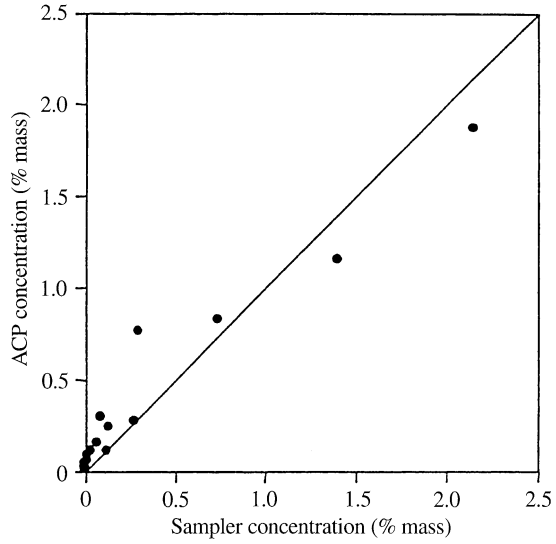

Fig. 7. Comparison of concentrations gathered with the ACP and the suction samplers without the attenuation corrected. 580 μm sand grain diameter

sediment are more erratic than vertical distributions of 120 μm sediment, and the equations developed for the ACP behave better for distributions of sediment that are more homogeneous. A significant portion of the error observed in Figs. 6 and 7 may be incurred by misalignment of the ACP and transmission tube. Consequently, in situ sediment samples for confirmation of the ACP calibration are always desirable.

The concentration profiles gathered in the experimental flume during the steady flow tests are given in Figs. 8 and 9 for the 120 and 580 μm sediment, respectively. Although the height of the ACP's measuring volume is 7.5 mm, the spatial resolution of the ACP is higher. In other words, the center of the measuring volume can be located quite accurately. For the profiles shown in Figs. 8 and 9, a spacing of 2.5 mm has been chosen as the distance between measurements, and the corresponding measuring volumes overlap somewhat.

The ACP can also be used to measure concentrations in unsteady flows. Figure 10 shows mean concentration measurements of 120 μm sand at various elevations above the bed as a function of time for an unsteady flow. The velocity pulse associated with the entrainment of the sediment is also shown in the figure. Large fluctuations in instantaneous concentration are typical since a majority of sediment entrainment is

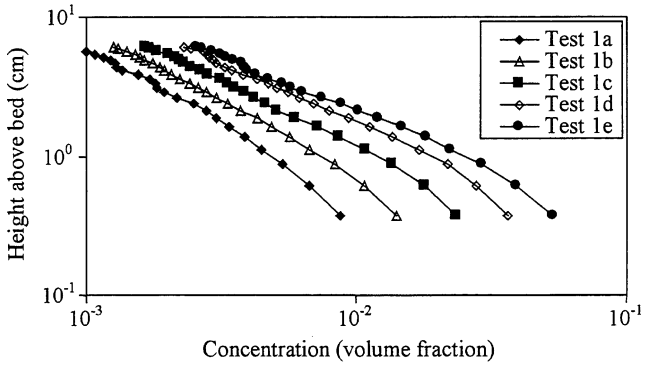

Fig. 8. Concentration profiles for 120 μm diameter sand tests

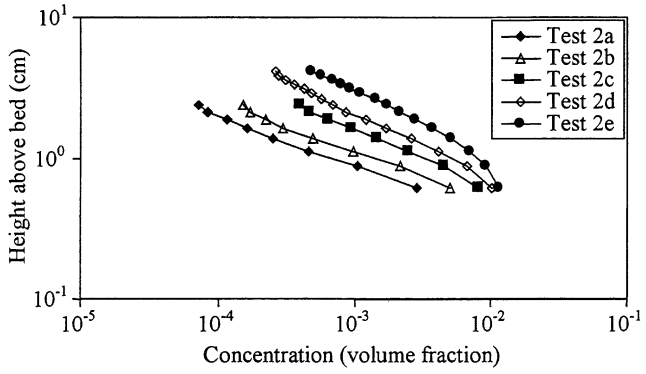

Fig. 9. Concentration profiles for 580 μm diameter sand tests

associated with turbulent events. Consequently, each unsteady experiment was repeated a large number of times, and the results were ensemble averaged. The centerline velocity and concentrations shown in Fig. 10 are ensemble averages of 60 realizations. A significantly larger number of realizations would be necessary to smooth out the concentration curves completely.

As long as the time required for the ACP to gather a sediment concentration profile is much less than the time it takes for the flow field to significantly change, the unsteadiness

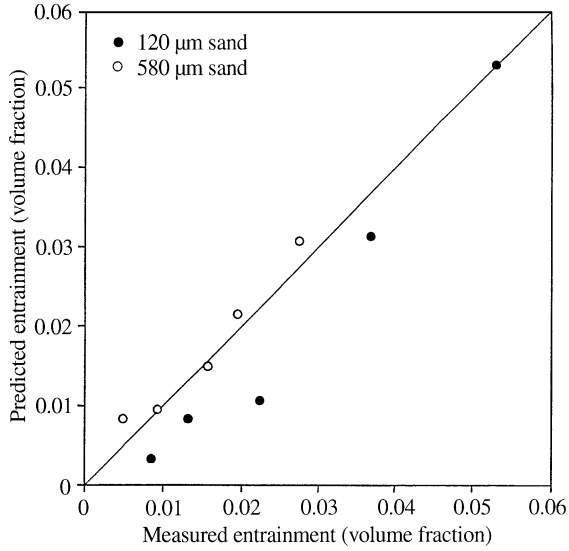

Fig. 11. Comparison of measured and predicted entrainment for steady flow tests

of the flow should not significantly affect operation of the ACP. For the current experiments the time necessary for gathering a profile is on the order of 0.5 ms.

7 Comparison of experimental results with existing theory

In order to calculate aggradation or degradation of a moveable bed, it is necessary to determine the net vertical flux of sand from the bed. Near the bed, at a reference height b_0, the downward flux of sand is the product of concentration and fall velocity. The upward flux of sand at b_0 is called the entrainment. The entrainment can be made dimensionless by dividing it by the sand fall velocity. For steady, equilibrium flows the upward and downward fluxes of sand are the same, and at b_0 the dimensionless entrainment and concentration are equal, as shown by

$$E_s|_{b_0} = \bar{c}|_{b_0} \tag{16}$$

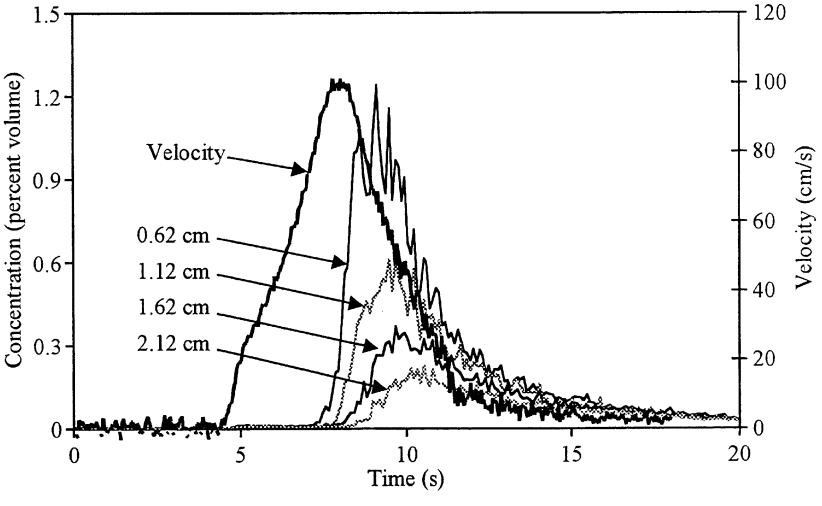

Fig. 10. Time variation of concentrations of 120 μm sand entrained by a velocity pulse

Table 3. Pulse flow test conditions

Test	Sand diameter [μm]	R_{ep}	Number of realizations	Peak velocity [cm/s]	Velocity pulse duration [s]	Entrainment time lag [s]
3a	120	4.85	60	101	7.5	0.53
3b	120	4.85	60	104	15.0	0.72
3c	120	6.11	100	96	3.45	0.26
3d	120	6.05	100	142	4.6	0.29
3e	120	6.09	100	139	2.72	0.03
4a	580	52.5	60	186	4.39	0.06
4b	580	54.0	80	141	7.9	0.12
4c	580	52.5	60	153	15.7	0.29

where E_s and $\bar{c}$ are the dimensionless entrainment and average concentration, respectively.

García and Parker (1991) developed the empirical relation given by Eq. (17) for calculating the entrainment at a reference level, b_0, of 1/20th of the flow depth:

$$E_s = \frac{AZ_u^5}{1 + \frac{A}{0.3}Z_u^5} \tag{17}$$

The coefficient A is equal to 1.3×10^{-7} and Eq. (18) defines the entrainment parameter, Z_u.

$$Z_u = \frac{u'_*}{v_s} R_{ep}^{0.6} \tag{18}$$

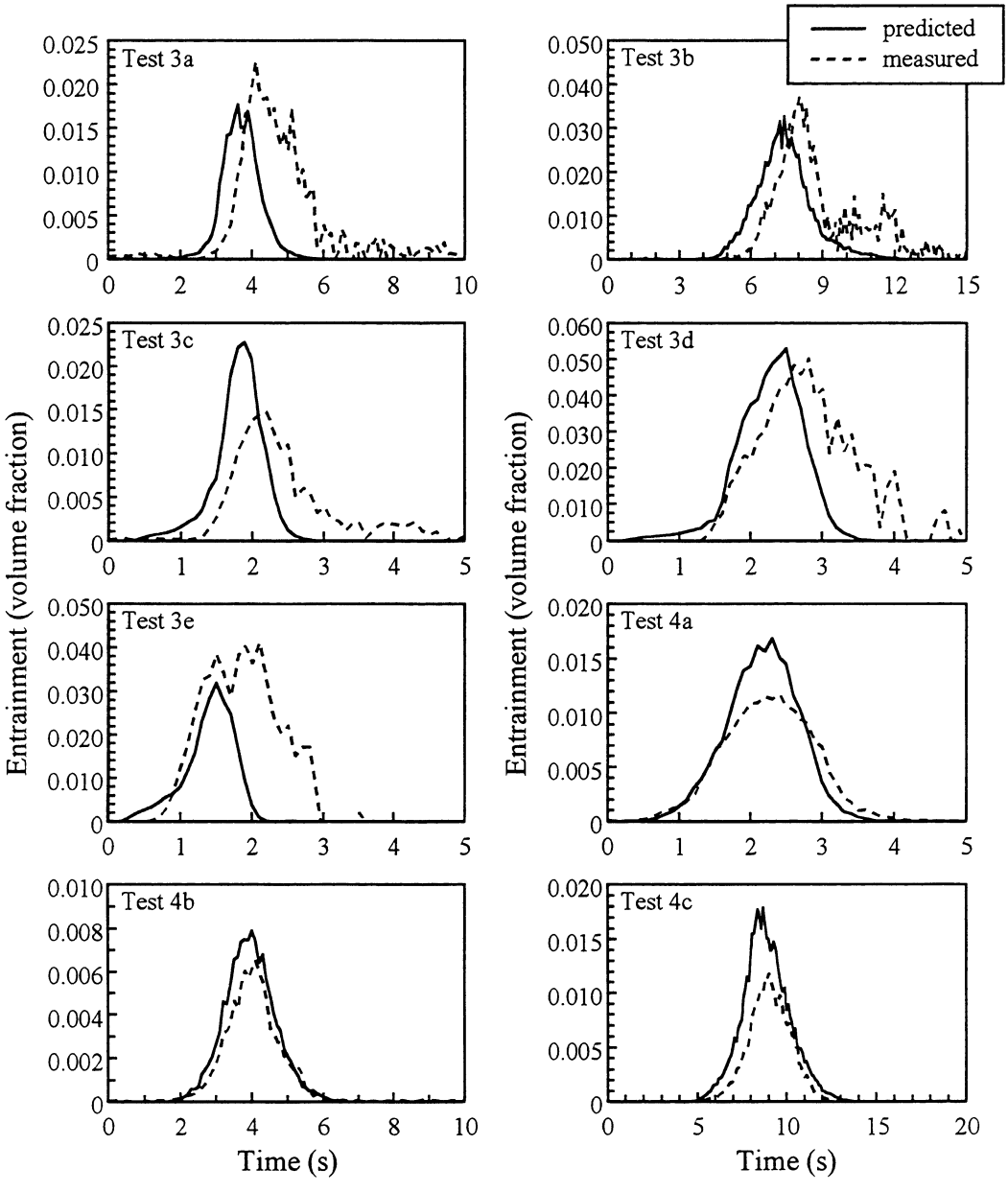

Fig. 12. Time series showing comparisons of measured and predicted entrainment for unsteady flow tests

where u'_* is the shear velocity based on the skin friction, v_s is the sand fall velocity (the assumption is made that fall velocity is a constant), and R_{ep} is the particle Reynolds number given by

$$R_{ep} = \frac{\sqrt{gRD_s}D_s}{v} \tag{19}$$

where g is the gravitational acceleration, R is the submerged specific gravity of the sediment (the specific gravity of the sediment minus the specific gravity of water), D_s is the mean sediment diameter, and v is the kinematic viscosity of the water. Using Eqs. (17)–(19) and the values of shear velocity and particle Reynolds number shown in Table 2, entrainment was calculated for all of the steady flow tests. Figure 11 gives a comparison of the near-bed concentration measured with the ACP, and the calculated values of entrainment.

For uniform, unsteady flows Admiraal (1999) has shown that the entrainment is not equal to the near-bed concentration, and that the entrainment must be calculated using Eq. (20):

$$\int_{t_0}^{t_1} E_s|_{b_0}\,\mathrm{d}t = \left(\frac{1}{v_s}\int_{b_0}^{b_1}\tilde{c}|_{t_0}^{t_1}\,\mathrm{d}z + \int_{t_0}^{t_1}\tilde{c}|_{b_0}\,\mathrm{d}t\right) \tag{20}$$

where z represents height above the bed, and the values b_0 and b_1 represent the lower and upper limits of the concentration profile, respectively. The lower limit of the profile is the same as the near-bed reference height. Entrainment is calculated for the time span bounded by the times t_0 and t_1. The tilde above the concentration indicates that the concentration is ensemble averaged. The entrainment given by Eq. (20) can be solved for as a function of time since the ACP rapidly gathers entire concentration profiles. However, for highly unsteady flows a large number of realizations are necessary.

A set of eight unsteady flow tests were performed in the experimental resuspension flume. In each of the tests the water in the flume was accelerated to a peak velocity and then decelerated to zero velocity. The rates of acceleration and deceleration were approximately constant. Each test consisted of a large number of realizations. Details of the tests are given in Table 3. Equation (20) was used to compute the entrainment measured with the ACP as a function of time, and Eq. (17) and shear stress measurements were used to predict the entrainment. Comparisons of the measured and predicted entrainment rates are shown in Fig. 12. Although Eq. (17) was originally developed for use with steady flows, predicted entrainment rates agree well with entrainment rates computed from ACP measurements except for a time lag. The delay between the time when peak shear stress occurs and the time when peak entrainment occurs is because of the time required for sediment to be transported from the bed into suspension. Time lags estimated for each of the tests are shown in Table 3. Entrainment predictions and ACP measurements appear to agree quite well for both steady and unsteady flows.

8 Conclusions

The ACP is able to non-intrusively gather entire concentration profiles at fairly high resolution. The results presented show that the ACP performs quite well, even with external calibration. The ACP performs better for finer sediment sizes since suspensions of fine sediment are usually more homogeneous, and temporal fluctuations in concentration are reduced. This is especially important for the data presented in this paper since the ACP's measuring volume is large relative to the height of the boundary layer. Coarse sediment, which does not get suspended into the flow as easily, has a steep concentration gradient near the bed. Consequently, it is much more difficult to measure concentrations of coarse sediment with the ACP.

As stated by Hay (1991) and shown in Fig. 6, at volume concentrations of greater than one percent, attenuation corrections become increasingly important, at least for the 120 μm sand. Average concentration measurements of greater than 1% by volume were not available for the 580 μm sand and attenuation corrections were unnecessary. Concentration fluctuations are higher for the 580 μm sand than for the 120 μm sand, and if concentration fluctuations are large, the measurable mean concentration is less since the ACP has a limited output range.

Although no direct measurements are available to confirm that the ACP measures sediment concentrations as accurately in unsteady flows as it does in steady flows, theory of ACP operation and unsteady flow measurements imply that there is no loss of accuracy as long as the time associated with changes in the flow is significantly less than the time it takes to gather the concentration profile. Since the time it takes to gather a concentration profile is extremely small, the ACP works well in most unsteady flows of interest in sediment transport. Comparisons of measured and predicted entrainment demonstrate the ACP's capability of measuring sediment concentration in unsteady flows.

References

Admiraal DM (1999) Entrainment of sediment by unsteady turbulent flows. Ph.D. Thesis. University of Illinois at Urbana-Champaign. Urbana, Illinois

Bosman JJ; Van der Velden ETJM; Hulsbergen CH (1987) Sediment concentration measurement by transverse suction. Coastal Eng 11: 353–370

Coleman NL (1981) Velocity profiles with suspended sediment. J Hydraulic Res 19: 211–229

Crawford AM; Hay AE (1993) Determining suspended sand size and concentration from multifrequency acoustic backscatter. J Acoust Soc Am 94: 3312–3324

Downing A; Thorne PD; Vincent CE (1995) Backscattering from a suspension in the near-field of a piston transducer. J Acoust Soc Am 97: 1614–1620

Fisher FH; Simmons VP (1977) Sound absorption in sea water. J Acoust Soc Am 62: 558–564

García MH; Parker G (1991) Entrainment of bed sediment into suspension. J Hydraulic Eng 117: 414–435

Hay AE (1991) Sound Scattering from a particle-laden turbulent jet. J Acoust Soc Am 90: Pt. 1. pp 2055–2074

Hay AE; Sheng J (1992) Vertical profiles of suspended sand concentration and size from multifrequency acoustic backscatter. J Geophys Res 97: 15,661–15,677

Libicki C; Bedford KW; Lynch JF (1989) The interpretation and evaluation of a 3-MHz acoustic backscatter device for measuring benthic boundary layer sediment dynamics. J Acoust Soc Am 85: 1501–1511

Shen C; Lemmin U (1996) Ultrasonic measurements of suspended sediments: a concentration profiling system with attenuation compensation. Measurement Sci Technol 7, pp. 1191–1194

Thorne PD; Hardcastle PJ; Hogg A (1996) Observations of near-bed suspended sediment turbulence structures using multifrequency acoustic backscattering, In: Coherent Flow Structures in Open Channels, eds PJ Ashworth; SJ Bennett; JL Best; SJ McLelland, New York: Wiley

Thorne PD; Holdaway GP; Hardcastle PJ (1995) Constraining acoustic backscatter estimates of suspended sediment concentration profiles using the bed echo. J Acoust Soc Am 98: 2280–2288

Thorne PD; Hardcastle PJ; Soulsby RL (1993) Analysis of acoustic measurements of suspended sediments. J Geophys Res 98: 899–910

Thorne PD; Campbell SC (1992) Backscattering by a suspension of spheres. J Acoust Soc Am 92: Pt. 1, 978–986

van Rijn LC (1981) Entrainment of fine sediment particles; development of concentration profiles in a steady, uniform flow without initial sediment load. Report on model investigation, Delft Hydraulics Laboratory M1531 Part II

Winterstein TA; Stefan HG (1983) Suspended sediment sampling in flowing water: Laboratory study of the effects of nozzle orientation, withdrawal rate, and particle size. University of Minnesota, St. Anthony Falls Hydraulic Laboratory. External memorandum No. M-168.